This is a repository copy of *The dental calculus metabolome in modern and historic samples*.

1 **Title**

2 The dental calculus metabolome in modern and historic samples

3

4 **Keywords:**

5 Metabolomics; dental plaque; oral microbiome; archaeology; GC-MS; UPLC-MS/MS

6

Abstract

Introduction: Dental calculus is a mineralized microbial dental plaque biofilm that forms throughout life by precipitation of salivary calcium salts. Successive cycles of dental plaque growth and calcification make it an unusually well-preserved, long-term record of host-microbial interaction in the archaeological record. Recent studies have confirmed the survival of authentic ancient DNA and proteins within historic and prehistoric dental calculus, making it a promising substrate for investigating oral microbiome evolution via direct measurement and comparison of modern and ancient specimens.

Objective: We present the first comprehensive characterization of the human dental calculus metabolome using a multi-platform approach.

Methods: Ultra performance liquid chromatography-tandem mass spectrometry (UPLC-MS/MS) quantified 285 metabolites in modern and historic (200 years old) dental calculus, including metabolites of drug and dietary origin. A subset of historic samples was additionally analyzed by high-resolution gas chromatography-MS (GC-MS) and UPLC-MS/MS for further characterization of metabolites and lipids. Metabolite profiles of modern and historic calculus were compared to identify patterns of persistence and loss.

Results: Dipeptides, free amino acids, free nucleotides, and carbohydrates substantially decrease in abundance and ubiquity in archaeological samples, with some exceptions. Lipids generally persist, and saturated and mono-unsaturated medium and long chain fatty acids appear to be well-preserved, while metabolic derivatives related to oxidation and chemical degradation are found at higher levels in archaeological dental calculus than fresh samples.

Conclusions: The results of this study indicate that certain metabolite classes have higher potential for recovery over long time scales and may serve as appropriate targets for oral microbiome evolutionary studies.

1. Introduction

Metabolites are small molecular weight molecules produced by a diverse range of enzymatic and chemical reactions, and include products derived from both endogenous and exogenous sources. Profiling metabolites in biological systems to define a metabolome is increasingly common, as it can provide insight into normal and perturbed metabolic processes and their relation to health and disease. Easily obtained human biofluids including serum (Psychogios et al. 2011), urine (Bouatra et al. 2013), and saliva (Dame et al. 2015) have been extensively profiled to define the range of metabolites that are produced in health, and how their levels fluctuate based on changes in activity (Daskalaki et al. 2015), diet (Lankinen et al. 2014), drug use (Fleet et al. 2008; Hahn et al. 1972), and disease progression (Yan et al. 2008). These studies have made it possible to search for specific metabolites that can act as biomarkers for a diverse range of disorders and diseases, including cardiovascular disease (Jensen et al. 2014), diabetes (Sysi-Aho et al. 2011), periodontal disease (Barnes et al. 2011; 2009), and cancer (Beger 2013).

Saliva has become an increasingly popular source for metabolite analysis because collection is simple, non-invasive, does not require training, and it is abundant and easy to resample and store (Dame et al. 2015). Saliva is composed mainly of water, but it also contains a wealth of molecules including mucins, proteins, carbohydrates, salts, and metabolites derived from serum, local cellular processes, diet, and oral microbes (Zhang et al. 2012). Because of the presence of serum-derived molecules, saliva has been used to search for biomarkers both of local diseases, such as periodontal disease (Barnes et al. 2011) and oral cancer (Yan et al. 2008), and also systemic diseases such as pancreatic and breast cancers (Sugimoto et al. 2010), and cardiovascular disease (Foley et al. 2012).

Metabolites from dental plaque, a microbial biofilm that develops on teeth, may provide novel information regarding host-microbiome interactions in health and disease. Dental plaque is likely to contain host saliva- and gingival crevicular fluid (GCF)-derived metabolites in addition to microbial metabolites, potentially providing a substrate for direct comparison of host and microbial activities. For reasons not well understood, dental plaque periodically and rapidly mineralizes to form dental calculus, a substance with concrete-like hardness that is immediately re-colonized by oral bacteria in a repetitive process (White 1991). Such rapid entombment has the potential to trap biomolecules from GCF and saliva as well as oral plaque and dietary and environmental debris (Warinner 2016; Warinner et al. 2015).

Although generally kept to low levels by professional dental hygiene regimens today, dental calculus was ubiquitous and relatively abundant in past human populations, as attested by dental calculus preserved within archaeological and paleontological collections spanning tens of thousands of years, and it is also found on the dentitions of some animal species (Warinner 2016; Warinner et al. 2015). Recent biomolecular investigations of ancient dental calculus have demonstrated that it contains exceptionally well preserved DNA and proteins from oral biofilm species, dietary components, and the host (Warinner, Hendy, et al. 2014; Warinner, Rodrigues, et al. 2014), as well as preserved plant microfossils (e.g., pollen, starch granules) and metabolic products (e.g, terpenoids) likely originating from dietary and craft activities (Blatt et al. 2011; Buckley et al. 2014; Hardy et al. 2012; Radini et al. 2016; Warinner, Rodrigues, et al. 2014). Such samples allow deep-time genetic and non-genetic molecular anthropology approaches to studying changes in human behavior, evolution of the oral biofilm and disease processes, and co-evolution of the oral microbiome and host, which are difficult to study using current *in vitro* and *in vivo* technologies alone. Gas-chromatography analyses of dental calculus from Neanderthals

3

79 (Buckley et al. 2014; Radini et al. 2016), pre-agriculturalists (Hardy et al. 2016), and early
80 agriculturalists (Hardy et al. 2012) have been used to infer the use of dietary and/or medicinal
81 plants; however, to our knowledge, no broad-scale analysis to determine the potential range of
82 metabolites trapped in dental calculus has been undertaken.
83   Here we present an in-depth, metabolic analysis of a set of historic and modern dental
84 calculus samples using a combination of targeted and untargeted approaches to assess the range
85 of metabolites that can be extracted from calculus, and how well they persist and preserve over
86 time. We validated our results and performed targeted metabolite searches in a subset of historic
87 samples for a more thorough assessment of the potential preservation of metabolites of interest.
88

2. Materials and Methods

2.1 Calculus collection and preparation

91   Fresh dental calculus samples were obtained during routine dental cleaning at the
92 University of Oklahoma Periodontology Clinic (n=1) in Oklahoma City, Oklahoma, USA and at
93 a private dentistry practice (n=4) in Jaen, Spain (Table 1). Samples were collected by dental
94 professionals using a dental scaler following standard calculus removal procedures. All samples
95 were obtained under informed consent, and this research was reviewed and approved by the
96 University of Oklahoma Health Sciences Center Institutional Review Board (IRB# 4543).
97 Historic dental calculus (Figure S1a) was collected from 12 skeletons in the Radcliffe Infirmary
98 Burial Ground collection, housed at Oxford Archaeology in Oxford, UK (Table 1). This
99 cemetery was used from 1770-c.1855, and the skeletons are not personally identifiable. The oral
100 health of each skeleton was recorded with reference to the presence or absence of caries and
101 periodontal disease, with reference to (Hillson 1996; Ogden 2005). The sex and approximate age
102 at death for each skeleton was estimated following standard osteological criteria (Brooks and
103 Suchey 1990; Buckberry and Chamberlain 2002; Ferembach et al. 1980; Lovejoy et al. 1985;
104 Phenice 1969; Schwartz 1996) and is presented in Table 1. Genetic sex was further confirmed
105 through high-throughput sequencing (HTS) of DNA extracted from additional calculus
106 fragments (described below) following previously described methods (Frantz et al. 2016;
107 Skoglund et al. 2015; 2013); genetic sex determinations for all twelve samples were consistent
108 with those made using osteological approaches. For details see Supplemental Methods.
109   After collection, the fresh and historic dental calculus samples were stored frozen and
110 transferred on dry ice to Metabolon, Inc. (Durham, NC) for sample processing and metabolite
111 extraction and detection by UPLC-MS/MS. A subset of five historic dental calculus samples
112 (CS6, CS12, CS18, CS24, and CS46) were additionally analyzed at the Departments of
113 Chemistry and Biomolecular Chemistry at the University of Wisconsin (Madison, USA) to
114 further characterize metabolites and lipids by high-resolution gas chromatography (GC)-MS and
115 UPLC-MS/MS (Table 1).
116

2.2 Genetic Authentication of a Preserved Oral Microbiome in Historic Samples

118   DNA extracted from a separate fragment of each piece of historic calculus was used to
119 assess microbial community composition. DNA was extracted as previously described, but
120 omitting phenol-chloroform steps (Warinner, Rodrigues, et al. 2014), and Illumina shotgun
121 sequenced (for details see Supplemental Methods). The 16S rRNA gene-identified reads were
122 then used to assess microbial community composition at the genus level by closed-reference
123 OTU-picking against the GreenGenes v. 13.8 database using UCLUST (Edgar 2010) in QIIME
124 v. 1.9 (Caporaso et al. 2010). The Bayesian analysis-based program SourceTracker (Knights et

125 al. 2011) was used to estimate the source composition of the microbial community identified by
126 QIIME. Human reads were identified by mapping to GRCh38.p10 (GCF_000001405.36) using
127 bwa (Meyer et al. 2012) with the flags aln -l 16500 -o 2 -n 0.01, duplicate reads were removed,
128 and reads mapping to X and Y chromosomes were analyzed for genetic sex determination as
129 described above.
130

131 *2.3 Mass spectrometry and data processing for UPLC-MS/MS*
132   Samples (~20 mg) were decalcified in 0.5M EDTA, centrifuged to pellet debris, and
133 supernatant prepared using the automated MicroLab STAR® system from Hamilton Company.
134 Samples were cleaned and divided into five fractions: two for analysis by two separate reverse
135 phase (RP)/UPLC-MS/MS methods with positive ion mode electrospray ionization (ESI), one for
136 analysis by RP/UPLC-MS/MS with negative ion mode ESI, one for analysis by HILIC/UPLC-
137 MS/MS with negative ion mode ESI, and one sample was reserved for backup. All methods
138 utilized a Waters ACQUITY ultra-performance liquid chromatography (UPLC) and a Thermo
139 Scientific Q-Exactive high resolution/accurate mass spectrometer interfaced with a heated
140 electrospray ionization (HESI-II) source and Orbitrap mass analyzer operated at 35,000 mass
141 resolution. For details see Supplemental Methods. Raw data were extracted, peak-identified and
142 QC processed using Metabolon's hardware and software. Compounds were identified by
143 comparison to library entries of purified standards or recurrent unknown entities. Peaks were
144 quantified using area-under-the-curve. Each compound was corrected in run-day blocks by
145 registering the medians to equal one (1.00) and normalizing each data point proportionately. For
146 specific details about the hardware, software, and libraries used, please see Supplementary
147 Materials section 2.6.
148

149 *2.4 Further characterization of historic calculus by GC-MS and UPLC-MS/MS*
150   Five historic dental calculus samples were selected to further investigate metabolites and
151 lipids in historic dental calculus samples (Table 1). Following sample pulverization, 15 mg was
152 decalcified with 100 uL of 4% Formic acid. Samples were incubated at 4˚C with occasional
153 shaking for 12 days. Next, 75 uL of 1 M ammonium hydroxide was added, then samples were
154 extracted with 350 uL MeOH + 350 uL Acetonitrile (final 2:2:1 Methanol:Acetonitrile:Water).
155 Extract was split for metabolite (GC-MS) and lipid (LC-MS) analysis and dried down by vacuum
156 centrifugation. For GC-MS analysis molecules were analyzed with electron-impact (EI)-Orbitrap
157 full scan of 50-650 m/z range. Lipid LC-MS analysis was performed on a Water's Acquity
158 UPLC CSH C18 Column (2.1 mm x 100 mm) with a 5 mm VanGuard Pre-Column Mobile
159 coupled to a Q Exactive Focus. Raw files were analyzed using an in-house tool for
160 deconvolution of spectra, quantitation, and identification against in-house and NIST 2014
161 libraries (GC-MS), or the Thermo Compound Discoverer[TM] 2.0 application with peak detection,
162 retention time alignment, and gap filling (UPLC-MS/MS). Only peaks 10-fold greater than
163 solvent blanks were included in the later analysis. The UPLC-MS/MS data was also processed
164 through the Global Natural Products Social Molecular Networking pipeline (Wang et al. 2016).
165 For details see Supplemental Methods.
166

167 *2.5 Data analysis*
168   Mass normalized data were used for all downstream analyses. Data was normalized as
169 follows: values for each sample were normalized by sample mass utilized for extraction, and
170 each biochemical was then rescaled to set the median equal to 1. Lastly, missing values were

171 imputed with the minimum. First, overall metabolome composition was summarized at the
172 super-pathway, sub-pathway, and metabolite levels, and identified metabolites were cross-
173 referenced against public databases to obtain KEGG compound identifiers and Human
174 Metabolome Database (HMDB) IDs. Next, metabolites found to be ubiquitously present in
175 modern samples and ubiquitously absent in historic calculus were compared. Here ubiquity
176 among the five modern samples was applied as a measure to identify highly prevalent
177 (potentially core) dental calculus metabolites; complete absence of these metabolites among all
178 twelve historic samples was used to identify metabolite candidates that may be particularly prone
179 to loss or that are unstable and susceptible to degradation through time-dependent taphonomic
180 processes. Following this analysis, differential representation of metabolites between historic and
181 modern samples was determined using the program Statistical Analysis of Metagenomic Profiles
182 (STAMP) (Parks and Beiko 2010; Parks et al. 2014), first including metabolites detected in both
183 historic and modern samples, and then again using only those metabolites that were universally
184 detected in all seventeen calculus samples. Metabolite profiles of historic and modern samples
185 were compared using 2 group analysis of the average quantity of each metabolite and analyzed
186 by White's non-parametric two-sided t-test with bootstrapping to determine the difference
187 between proportion (DP) with cut-off 95% and Storey's FDR. Differential abundance was
188 determined in hierarchical categorization of super-pathway, sub-pathway, and individual
189 metabolite. For both analyses corrected p-values (q-values) of ≤ 0.05 together with an effect size
190 ≥ 1 were considered significant. Pathway maps were created using iPATH2 (Yamada et al. 2011)
191 for metabolites with KEGG compound identifiers. Partial Least Squares Discriminant Analysis
192 (PLS-DA) was performed using the R package mixOmics (Rohart et al. 2017) in default settings,
193 and Q2 values for the PLS-DAs was calculated in the R package DiscriMiner
194 (https://github.com/gastonstat/DiscriMiner) using 2 components to match the mixOmics
195 calculations, and "leave one out" cross-validation.
196
197 **3 Results**
198
199 *3.1 Authentication of historic calculus*
200   Archaeological specimens are subject to environmental degradation and contamination,
201 and thus it is necessary to confirm of the source (e.g., endogenous microbiome vs. exogenous
202 environmental microbes) of biomolecules detected in ancient samples. QIIME and
203 SourceTracker analyses confirmed excellent biomolecular preservation of an *in situ* oral
204 microbial community within the historic dental calculus samples, and16S rRNA gene sequences
205 closely matched those expected for dental plaque communities, with minimal contamination
206 from exogenous sources such as soil and skin (Figure S1b). The high proportion of microbes of
207 "unknown" source in several historic dental calculus samples is observed in modern calculus
208 samples (Ziesemer et al. 2015) (Figure 1b 'Modern'), and is a result of mismatched source
209 samples. Several poorly taxonomically characterized oral taxa such as *Methanobrevibacter* and
210 *Tissierellaceae* are highly abundant in mature dental calculus biofilms but are infrequently
211 detected in healthy oral plaque early biofilms such as the Human Microbiome Project cohort we
212 used as source samples. Therefore these genera cannot be confidently assigned to an oral plaque
213 source, and are instead attributed to an unknown source.
214
215 *3.2 Metabolic pathway coverage in dental calculus*

6

A total of 285 metabolites were identified by UPLC-MS/MS in the seventeen dental calculus samples, and these were categorized as members of one of eight super-groups: *Amino acids*, *Carbohydrates*, *Cofactors and vitamins*, *Energy*, *Lipids*, *Nucleotides*, *Peptides*, and *Xenobiotics* (Figure 1a; Supplemental Table S1), which were further classified into 69 sub-categories. More than half of the metabolites (n=185) were detected in both historic and modern calculus samples, demonstrating that metabolites can be recovered from historic dental calculus, while 99 metabolites were detected only in modern samples and 1 was detected only in historic samples. One hundred ninety-nine metabolites were detected in all 5 modern samples, 97 were detected in all 12 historic samples, and 85 were detected in all 17 calculus samples (Table S1). A smaller subset of historic calculus was analyzed by GC-MS and LC-MS at the University of Wisconsin-Madison; this enabled the identification of 15 additional metabolites and 40 additional lipids, respectively (Figure 1b; Table S2). For metabolites that were quantified in the main analysis and in the smaller subset, we see comparable quantitation despite differences in extraction procedures and analysis methods between Metabolon and the University of Wisconsin (positive correlation, $R^2 = 0.7$, Supplemental Figure S2). UPLC-MS/MS-identified metabolites with KEGG compound identifiers (n=207) were located on a general metabolic pathway map (Figure S3) and a map of biosynthesis of secondary metabolites (Figure S4).

To try to characterize more of the unknown features, we analyzed the LC-MS data acquired on the subset of historic calculus through the Global Natural Products Social Molecular Networking (GNPS) pipeline (Wang et al. 2016). This online tool searches experimental MS2 spectra against a large number of publically available spectral libraries and clusters spectra based on shared fragment ions. The identified clusters were primarily molecules that had been identified previously by Metabolon. Expectedly, we found molecular clusters associated with lipid class: for example, phosphatidylcholines clustered within the same molecular network, and these molecules shared network connections with sphingomyelins containing phosphocholine head groups (Figure S5). We also observed clusters of molecules that could be categorized as plasticizers, which had not been identified in the data set by metabolon; however, we suspect these molecules were introduced during sample processing. For example, one of these molecules - didodecyl 3,3′-thiodipropionate - has been previously reported to be leached from polypropylene tubes during organic extractions (Xia et al. 2005).

3.3 Comparison of dental calculus and saliva metabolomes

To determine the degree of overlap between metabolites in dental calculus and metabolites in saliva, we compared our results to the saliva metabolome. We downloaded a list of all metabolites reported in saliva as catalogued in the Human Metabolome Database (Wishart et al. 2013) version 3.6 (hmdb.ca) as of February 2017 to use as the known saliva metabolome. This list contained 1233 metabolites of endogenous and exogenous origin, spanning the full range of super-pathways detected in calculus samples. Just over half, 159, of the 285 metabolites detected in calculus (55.7%) were previously included in HMDB's saliva metabolome (Table S1), while these 159 metabolites make up just 12.9% of the total metabolites detected in saliva. Of the remaining 107 metabolites detected in calculus, 84 have been detected in blood, urine and/or cerebrospinal fluid, and 23 have no HMDB identifier. At least one metabolite in each of the sub-pathways represented in calculus is not included in the HMDB saliva metabolome.

3.4 Metabolite preservation patterns

7

261   Among metabolites that are likely endogenous (host or oral microbiome) in origin (i.e.,
262 not xenobiotics), metabolite persistence differs by super-pathway in historic samples (Figure 1).
263 Overall, historic samples had lower representation in metabolites categorized as *Amino acids*,
264 *Vitamins and cofactors*, *Carbohydrates*, *Nucleotides*, and *Peptides* (Figure 2a). In contrast,
265 *Lipids* and *Energy* metabolites were generally observed in both historic and modern calculus
266 (Figure 2a). Additionally, at a finer scale, certain chemical configurations appear to be lost
267 through time, for example N-acetylation, amino acids with positively-charged R-groups, and
268 phenyl rings one carbon away from an oxygen. These data suggested a preservation bias that
269 could be due to either chemical stability or compound solubility, although it is a possibility that
270 low sample amounts limit the detection of certain metabolites.
271   To test the hypothesis that preservation is linked to aqueous solubility, we compared the
272 differential abundance of metabolites between modern and historic calculus to the predicted
273 hydrophobicity of the compounds. The predicted hydrophobicity was extracted from the HMDB,
274 which sources the ALOGPS predicted ratio of compound partitioning between 1-octanol and
275 water (logP) (Tetko and Bruneau 2004). When plotting fold-change abundance (modern/historic)
276 to logP, we observe a significant ($p < 0.001$) negative correlation (Figure 2b), suggesting that
277 molecules that are more abundant in modern calculus have lower organic solubility and higher
278 aqueous solubility. This result is consistent with our hypothesis that metabolite preservation is in
279 part due to aqueous solubility. The exception to our hypothesis, and the outlier in Figure 2b, are
280 poly-unsaturated fatty acids (PUFAs), which have high logP but low preservation. Two PUFAs,
281 mead acid (20:3n9) and dihomo-linolenate (20:3n3 or n6), were identified in all modern dental
282 calculus samples but were not observed in historic samples. The loss of these PUFAs in historic
283 calculus may be partially explained by the decreased oxidative stability of fatty acids with
284 decreasing saturation (Cosgrove et al. 1987; Rustan and Drevon 2005).
285   As yet there are no detailed assessments of metabolite degradation in archaeological
286 dental calculus; however, analyses of protein damage patterns in human dental calculus and
287 mammoth bone (Cappellini et al. 2012) can be used to draw comparisons with damage patterns
288 in calculus metabolites. Warinner, *et al*. (Warinner, Rodrigues, et al. 2014) found that the most
289 common protein post-translational modification products in ancient dental calculus are
290 deamidation of asparagine, deamidation of glutamine, oxidation of methionine, and conversion
291 of N-terminal glutamine to pyroglutamate. Asparagine was detected in all five modern samples
292 and eleven historic samples, while the deamidation product aspartate was detected in all
293 seventeen samples, and in higher quantity. Glutamine was detected in all modern samples but not
294 in historic samples, and its deamination products glutamate and 5-oxoproline were detected in
295 higher concentration in all 17 samples, although at much higher concentration in modern than
296 historic samples. Oxidation, which is widely documented in the degradation of oil paintings
297 (Oakley et al. 2015) and food spoilage (Velasco and Dobarganes 2002) also occurs in dental
298 calculus. For example, the ratio of cholesterol and its oxidation product 7-ketocholesterol was
299 reversed between modern and historic calculus, and kynurenin, an oxidation product of
300 tryptophan that is known to accumulate in archaeological bone over time (Cappellini et al. 2012),
301 was detected in historic calculus while tryptophan was absent. In contrast, methionine was
302 detected in all seventeen samples, and was much more abundant in modern samples, while the
303 oxidation product methionine sulfoxide was detected in all five modern samples and in only two
304 historic samples, in all cases at lower concentrations. Free methionine sulfoxide may be unstable
305 and subject to further rapid breakdown.
306

3.5 Lipid 2-hydroxylation as an indicator of calculus age

Four 2-hydroxylated lipids were detected in all calculus samples—2-hydroxyadipate, 2-hydroxystearate, 2-hydroxypalmitate, and 2-hydroxyglutarate—and the first three are more abundant in ancient than modern samples. The only metabolite detected in historic but not modern samples was 2-hydroxydecanoate (detected in 10 of the 12 historic samples), while the parent molecule decanoate was not detected in any of our samples. In contrast, 3-hydroxylated and 2,3-hydroxylated lipids are more abundant in modern than historic samples. The increased presence of 2-hydroxylated lipids in ancient samples suggests that this modification may increase over time. The difference in patterns of lipid hydroxylation between ancient and modern calculus suggests that in some cases 3-hydroxylation may switch to 2-hydroxylation.

3.6 Differentially abundant metabolites in ancient and modern calculus

To further define the differences in metabolic functions preserved through time, we compared the metabolites present in both modern and ancient calculus samples at the super-pathway, sub-pathway, and individual metabolite levels using STAMP. Principal components analysis demonstrated distinct separation of modern and historic samples (Figure 3a) with tight clustering of historic samples along PC1 and PC2, while modern samples were more distributed, suggesting that loss of metabolites through time results in a more uniform metabolite profile between samples than may have originally existed. Comparing the mean proportions of individual metabolites detected in at least one modern and one historic sample, 161 were significantly more abundant ($q \leq 0.05$) in one sample set, yet only 21 additionally had an effect size of ≥ 1.0 (Figure 3b, Table S3 bold metabolites). When considering only the metabolites that were universally present in all five modern and all twelve historic samples (Table S3, superscript 'c'), a slightly different set of metabolites and metabolic pathways are differentially abundant. Historic and modern samples still separate distinctly in PCA (Figure S6a), but many more metabolites have a significant difference in mean proportions (Figure S6b).

We then examined differences in proportion of super-pathways, sub-pathways, and individual metabolites present in at least one modern and historic sample to better understand the patterns of preservation and loss through time. The proportion of *Lipids* was significantly higher in ancient than modern calculus samples, suggesting that non-polar, chemically inert molecules are particularly stable through time (Figure 4a). On the other hand, the proportion of *Amino acids*, *Carbohydrates*, *Cofactors and vitamins*, and *Xenobiotic*s were significantly higher in modern calculus (Figure 4a), demonstrating substantial loss and/or degradation of metabolites in these super-pathways over time. The super-pathway *Peptides* was excluded from analysis using this method because its near total absence in historic samples resulted in very few possible comparisons.

As expected from the super-pathway differential abundances, many of the sub-pathways with greater proportional representation in historic calculus were related to lipid metabolism (Figure 4b). The sterols include cholesterol and its oxidation products 4-cholesten-3-one, 7-hydroxycholesterol (alpha or beta), and 7-ketocholesterol, which is consistent with the expectation that increased oxidation will occur over time. *Guanidino and acetamido metabolism* comprised a greater proportion of historic sample metabolites due to overrepresentation of 4-guanidinobutanoate, a product of arginine and putrescine metabolism. Several of the sub-pathways with greater proportional representation in modern samples can be explained by a single metabolite, which manifests at the metabolite level (Figure 4b), and these include *Nicotinate and nicotinamide metabolism*, *Pyrimidine metabolism*, and *Food component/plant*. A

9

353 single metabolite each comprises the *Chemical* and *Drug* sub-pathways, sulfate and salicylate,
354 respectively. With respect to the latter, salicylate is abundant in modern pharmaceuticals, but
355 may have been consumed medicinally in the form of willow bark tea by the historical population,
356 especially given the fact that they were buried in a hospital-associated cemetery. Salicylates are
357 also naturally found in a variety of fruits, vegetables, herbs, and spices; however at levels far
358 below the therapeutic doses typical of modern pharmaceuticals (Castillo-García et al. 2015).
359 Alternatively, the salicylates in the historic calculus samples may be a plant root-derived product
360 (Badri and Vivanco 2009), resulting from the diffusion highly soluble, small organic acids into
361 the calculus from burial soil.
362 　　　　In contrast to the large number of sub-pathways representing a significantly higher
363 proportion of metabolites between historic and modern calculus, only 6 individual metabolites
364 were significantly differentially represented between historic and modern calculus (Figure 4c).
365 Modern calculus had significantly higher proportions of nicotinate, orotate, stachydrine, alanine,
366 and glucose (Figure 4c). Both nicotinate and orotate may be taken as a dietary supplement, while
367 stachydrine (proline betaine), is a plant metabolite that is not metabolized by mammals (Lever et
368 al. 1994), but is common in citrus fruits and orange juice (Atkinson et al. 2007). Low abundance
369 of stachydrine in historic calculus may relate to dietary differences between these modern and
370 historic populations, or to differential preservation. Alanine, the smallest amino acid, and glucose
371 may be lost through high solubility. The lipid 2-hydroxystearate was the only metabolite of
372 significantly greater proportion in historic samples, even though several 2-hydroxylated lipids
373 had greater relative abundance in historic samples.
374 　　　　In addition to endogenous metabolites, several xenobiotics found to be present only in
375 modern calculus samples are from food and pharmacologic agents introduced to or popularized
376 in European populations in the 20th century, including the artificial sweeteners acesulfame,
377 saccharin, and arabitol/xylitol. Additionally, theobromine, an alkyloid present in coffee, tea, and
378 chocolate, was also only detected in modern calculus, suggesting that consumption of these
379 products by the historic population was absent or low, despite their increasing availability in
380 Europe in the 1800s, or that this metabolite poorly preserves over time.
381

3.7 Potential for maintenance of biological signatures in calculus metabolite profiles
383 　　　　Unlike saliva, dental calculus does not represent a snapshot of a specific time and specific
384 metabolic state, but rather it represents a life history in which specific profiles may be diluted out
385 by fluctuating metabolic processes throughout an individual's life, loss of unstable metabolites
386 over time, and random chance with respect to the entrapment of xenobiotics and dietary
387 compounds. However, distinct metabolic signatures related to biological variables such as sex
388 (Takeda et al. 2009), oral health status (Barnes et al. 2009; 2011), and oral biofilm microbial
389 composition (Takahashi et al. 2010) have been reported in saliva, GCF, and oral plaque samples,
390 all of which are likely to contribute to the metabolite profile in dental calculus. Therefore, we
391 assessed differences in metabolic profiles between calculus from different age groups, sex, and
392 oral health status by partial least squares discriminant analysis (PLS-DA) (Q2 valuesTable S4),
393 and, further, looked for metabolites that could be specifically attributed to bacterial activity.
394 　　　　No differences were found in the metabolite profile between age groups, between males
395 and females, between samples from caries-affected and caries-free dentitions, or between
396 samples from periodontal disease-affected and non-affected individuals when considering
397 metabolites detected in at least one historic and one modern calculus sample (Figure 5a), or
398 metabolites universally present in all 17 samples (Figure S8a). However, there was a distinct

10

399 separation of modern and historic samples in each comparison so we repeated PLS-DA using
400 only historic sample data. PLS-DA separated historic samples based on sex, age, caries status
401 and periodontal disease status when using metabolites detected in at least one historic sample
402 (Figure 5b) and when using only metabolites present in all 12 historic samples (Figure S8b).
403 Applying PSL-DA to universally detected metabolites in only the *Lipid* and *Energy* classes, (the
404 best-preserved classes in historic samples, Figure 1a) separated samples based on time period
405 rather than biological category (Figure S8c). These results suggest that biological categories in
406 modern and historic calculus samples cannot be directly compared, yet patterns of biological
407 differences are maintained through time.

408 Similarly, no metabolites could be specifically attributed to bacterial processes, but
409 several metabolites, including isovalerate, valerate, lactate, cadaverine and putrescene, are
410 known metabolic products of oral bacteria (Scully et al. 1997; Takahashi 2015). Dipicolinate,
411 which was detected in all modern and all historic samples, is the major component of bacterial
412 spore capsules, and may indicate that bacterial endospore development occurs in mature plaque
413 biofilms, or during plaque mineralization. Sulfate is abundant in GCF due to break-down of
414 sulfur-containing amino acids by the oral biofilm, and is produced during anaerobic
415 methanogenesis in oral plaque, however, we observed no correlation between the relative
416 abundance of the oral methanogen *Methanobrevibacter* and sulfate levels (Figure S9) in our
417 samples, and the very high abundance of sulfate in historic relative to modern calculus suggests
418 an exogenous source. Oxford topsoil sulfur concentrations where the cemetery was located are in
419 the 70th percentile across England and Wales (Rawlins et al. 2012), and sulfates in the soil and
420 ground water of the cemetery may leach into the calculus by the same processes through which
421 highly water-soluble metabolites are leached out of calculus.

4 Discussion

424 Our results derived from the non-targeted assessment of metabolites present in dental
425 calculus from both modern and historic samples demonstrate the significant potential of calculus
426 as a material for metabolomics and lipidomic studies. The wide range of metabolic categories
427 covered (amino acids, carbohydrates, cofactors and vitamins, energy, lipids, nucleic acids,
428 peptides, xenobiotics), and the variety of sources of metabolites (host, microbial, diet) are on par
429 with those reported in saliva (Barnes et al. 2011) and GCF (Barnes et al. 2009) using similar
430 metabolite detection platforms. Similar to the study defining the saliva metabolome (Dame et al.
431 2015), we found using multiple metabolomics platforms (5 different methods by Metabolon, Inc.
432 and 2 by UW-Madison) increased the diversity of compounds we detected. However, unlike
433 Dame *et al* (2015), we found more metabolites by LC than GC methodologies, which was likely
434 due to the low-abundance of molecules with higher aqueous solubility in the historic calculus
435 that were analyzed by GC-MS. Although we found lower representation of aqueous-soluble
436 molecules, in general calculus preserves a wide variety of molecules from the oral cavity and
437 could be useful proxy for oral biofluids in archaeological samples. Calculus also provides an
438 opportunity to co-investigate host and microbial activity, which is increasingly recognized as
439 important to understanding cellular physiology and disease pathology (Takahashi 2015).

440 Saliva has been shown to preserve an individualized metabolic signature throughout daily
441 routine (Wallner-Liebmann et al. 2016) and dental calculus, which contains salivary components,
442 has the potential to preserve aspects of individual profiles over longer periods of time. While
443 only five modern calculus samples were included in this study, PCA analysis revealed substantial
444 metabolite profile diversity within these samples (Figure 2a). It therefore appears that modern

11

445 calculus may preserve individual phenotypes, although to investigate this, studies with larger
446 sample sizes are needed to further assess this potential. Historic samples, in contrast, cluster
447 much more tightly in the PCA, suggesting that individual phenotypes may be lost through
448 metabolite degradation and loss over time. However, we were able to distinguish metabolic
449 profile differences in historic samples between sex, age, and oral health status of the individuals
450 by PLS-DA, demonstrating maintenance of individual profiles despite metabolite loss. It may
451 then be possible to investigate differences in specific metabolite profile in historic samples,
452 which could contribute to our understanding of disease demographics and evolution.

453 Relatively little is known about the process of age-related protein degradation in
454 archaeological samples, yet other historic samples provide some insight. Asparagine readily
455 deamidates via cyclization to succinimidyl within chain; however, this mechanism is unavailable
456 to the free amino acid. Under experimental heating, asparagine undergoes rapid hydrolysis (Crisp
457 et al. 2013), and it is therefore probable that the free asparagine seen in the historic samples is
458 derived from hydrolysis of peptides. Free glutamine and glutamic acid can undergo cyclisation to
459 pyroglutamic acid even at low temperatures (Nagana Gowda et al. 2015). However, although
460 pyroglutamate (pGlu; 5-oxoproline) is present at higher levels in the historic samples, it is too
461 low to account for all the loss of all glutamic acid. This consistent pattern suggests that there is a
462 contributing pool of degrading proteins, generating free amino acids which are undergoing
463 modification, either in chain (e.g., asparagine deamidation) or once hydrolysed to terminal
464 positions or as free amino acids (e.g., pyroglutamate). The majority of these low molecular
465 weight, high solubility products are then likely lost from the calculus matrix. It is possible that
466 some are so entrapped within the crystal matrix that they may persist as free amino acids and
467 pyroglutamate, and this could be assessed by monitoring the level of racemization (Crisp et al.
468 2013).

469 Persistence of the Energy metabolites is unexpected given that most of the molecules in
470 this category are small and water soluble, and therefore expected to be lost through time. Alpha-
471 ketoglutarate may be produced by degradation of glutamate, which appears to be occurring in
472 calculus as discussed in our results, and it may form stabilizing complexes with calcium, which
473 is highly abundant in the predominantly calcium-phosphate mineral matrix of dental calculus.
474 However, we speculate that these Energy metabolites may be fungal- or plant-derived
475 compounds from the burial soil. Both plant roots and their associated mycorrhizal fungi secrete
476 organic acids including citrate, malate, and oxalate (Badri and Vivanco 2009; Klugh and
477 Cumming 2007), which are more abundant than expected in our historic samples. We expect that
478 the endogenous Energy metabolites are lost over time through solubility, yet organic acids
479 present in the soil from roots and fungi may diffuse into the historic calculus samples, and thus it
480 appears that these metabolites are not lost through time. This concern may be addressed in future
481 experiments by looking at preservation of small organic acids in historic calculus samples from
482 individuals who were never buried in soil, such as from crypt burials, and from archaeological
483 samples that have been in storage for varying periods of time.

484 Lipids, particularly unmodified, saturated classes, are some of the best-preserved
485 metabolites in historic calculus, and appear to be particularly stable over time. Therefore, lipid
486 analyses may be a promising focus for historic calculus studies. Although not a common focus in
487 salivary or oral biofilm metabolomics studies, lipids are a versatile class of molecule with a
488 broad range of physiological properties and actions. They play roles in local (intracellular)
489 (Nishizuka 1995) and long-distance (hormone) cell signaling (Xavier et al. 2016), have both pro-
490 and anti-inflammatory properties (Bennett and Gilroy 2016), and are the major components of

cell membranes, where their composition influences cell membrane function (Zalba and Hagen 2017). Bacterial membrane lipid content varies by species (López-Lara and Geiger 2016), and may indicate bacterial physiological status (Darveau et al. 2004), while pathogenesis of the periodontal disease-associated oral bacteria *Porphyromonas gingivalis* is influenced by host cell membrane lipid composition (Min Wang and Hajishengallis 2008). The role of lipid mediators in the initiation and resolution of periodontal disease inflammation is currently under investigation (Bartold and Van Dyke 2013), and the wealth of lipids detected in calculus may be valuable to studies of both host and microbial pathophysiology.

Although we were unable to specifically identify bacterial contributions to the calculus metabolome, there are some metabolites suggestive of mature oral biofilm activity. Dipicolinate, which is the major capsule component of bacterial endospores, is a highly stable molecule, as evidenced by the long-term viability of endospores (Yung et al. 2007). To our knowledge, the inferred presence of endospores in calculus is a novel finding, as we were unable to find any references to the presence of bacterial endospores in oral plaque or dental calculus. Members of several Gram-positive genera that reside in the mouth have close relatives known to form spores, including *Actinomyces* (Gao and Gupta 2012), and *Filifactor* (Vos et al. 2011), and since many oral bacteria have not yet been genetically or physiologically characterized, it is possible that several oral species do have the ability to form spores. Calcification of the biofilm may induce a stress response in these species that initiates endospore formation, which would explain the abundance of dipicolinate in dental calculus.

Additionally, studies aiming to characterize salivary biomarkers of periodontal disease have identified several pathways with an apparent bacterial source that contain promising metabolite candidates for disease biomarkers (Kuboniwa et al. 2016; Sakanaka et al. 2017), and we have identified several of these in our calculus. Phenylalanine, succinate, hydrocinnimate, cadaverine, and putrescine are markers of periodontal disease that were reduced in saliva when supragingival plaque was removed, suggesting they were largely produced by bacteria (Sakanaka et al. 2017), and we detected each of these molecules. This demonstrates that bacterial metabolic products are present in calculus, and may offer insight into mature biofilm activity. This could be useful in studying how bacterial metabolism influences oral disease, as periodontal disease-associated oral plaque has community structure and activity much more similar to that of fully mature biofilms such as are found in calculus, than to healthy site subgingival plaque or supragingival plaque (Wade 2013), yet the presence of calculus alone is not a reflection of periodontal disease status (i.e., three of the five modern calculus samples were collected from teeth with no evidence of periodontal disease).

In sum, our results demonstrate that dental calculus contains an abundance of endogenous and exogenous metabolites, and that a wide range of these metabolites preserve well through time. Dental calculus therefore has significant potential to provide novel insights into human diet, physiology, and microbiome activity in both modern and historic samples, permitting human evolutionary and human-microbiome co-evolutionary studies with a deep-time perspective. Larger sample sizes and samples from additional temporal and cultural contexts as well as from varying burial and storage conditions are needed to further address metabolite preservation and presence/absence patterns. The excellent preservation of dental calculus in archaeological collections, however, means that there is ample opportunity to expand metabolite-based studies of dental calculus into the recent and distant past.

Acknowledgments

13

Compliance with ethical standards

Conflict of interest All authors declare that they have no conflict of interest.

Ethical approval The study was approved by the Institutional Review Board for Human Research Participant Protection at the University of Oklahoma [IRB#4543] and was performed in accordance with the 1964 Helsinki declaration and its later amendments.

Informed consent Informed consent was obtained from all modern participants in the study prior to the collection of dental calculus.

Data availability
All data generated or analyzed during this study are included in this published article (and its supplementary information files).

561 **Tables**

562

Table 1. Summary of sample demographic and health information and analyses performed

ID	Age[a]	Sex[b]	Smoker	Oral Health	Sampled Tooth	Analyses performed
Modern						
OK1010	40	M	Former	+ PD	- caries, + PD	UPLC-MS/MS
ES28	31	F	Current	+ caries, + GV	- caries, - PD	UPLC-MS/MS
ES29	30	M	No	+ caries, + GV	- caries, - PD	UPLC-MS/MS
ES20	23	M	Current	+ caries, + GV	- caries, - PD	UPLC-MS/MS
ES15	71	M	Former	+ caries, + PD	- caries, + PD	UPLC-MS/MS
Historic						
CS06	36-45	M	N/A	+ caries, + PD	- caries, - PD	UPLC-MS/ MS[d]; GC-MS
CS12	36-45	M	N/A	+ caries, + PD	- caries, - PD	UPLC-MS/MS[d]; GC-MS
CS18	36-45	M	N/A	- caries , + PD	- caries, - PD	UPLC-MS/MS[d]; GC-MS
CS24	36-45	F	N/A	+ caries, + PD	+ caries, + PD	UPLC-MS/MS[d]; GC-MS
CS46	>45	F	N/A	+ caries, + PD	- caries, - PD	UPLC-MS/MS[d]; GC-MS
CS20	36-45	M	N/A	+ caries, + PD	- caries, - PD	UPLC-MS/MS
CS21	26-35	M	N/A	- caries, - PD	- caries, - PD	UPLC-MS/MS
CS23	26-35	F	N/A	+ caries, + PD	- caries, - PD	UPLC-MS/MS
CS30	18-25	F	N/A	+ caries, - PD	- caries, - PD	UPLC-MS/MS
CS31	36-45	F	N/A	+ caries, + PD	- caries, - PD	UPLC-MS/MS
CS39	36-45	M	N/A	- caries, + PD	- caries, - PD	UPLC-MS/MS
CS40	>45	F	N/A	- caries, - PD	- caries, - PD	UPLC-MS/MS

[a]Age of skeletons used for historical calculus sampling is based on osteological indicators and is a range estimate. [b]Historical skeleton sex estimate is based on both osteological indicators and DNA sequencing, and was in concurrence between the two methods. [d]UPLC-MS/MS was performed twice; the first at Metabolon, Inc. and the second at the University of Wisconson-Madison. PD, periodontal disease; GV, gingivitis; N/A, not available; +, present; -, absent.

563

564

565   **Figure legends**

566

567
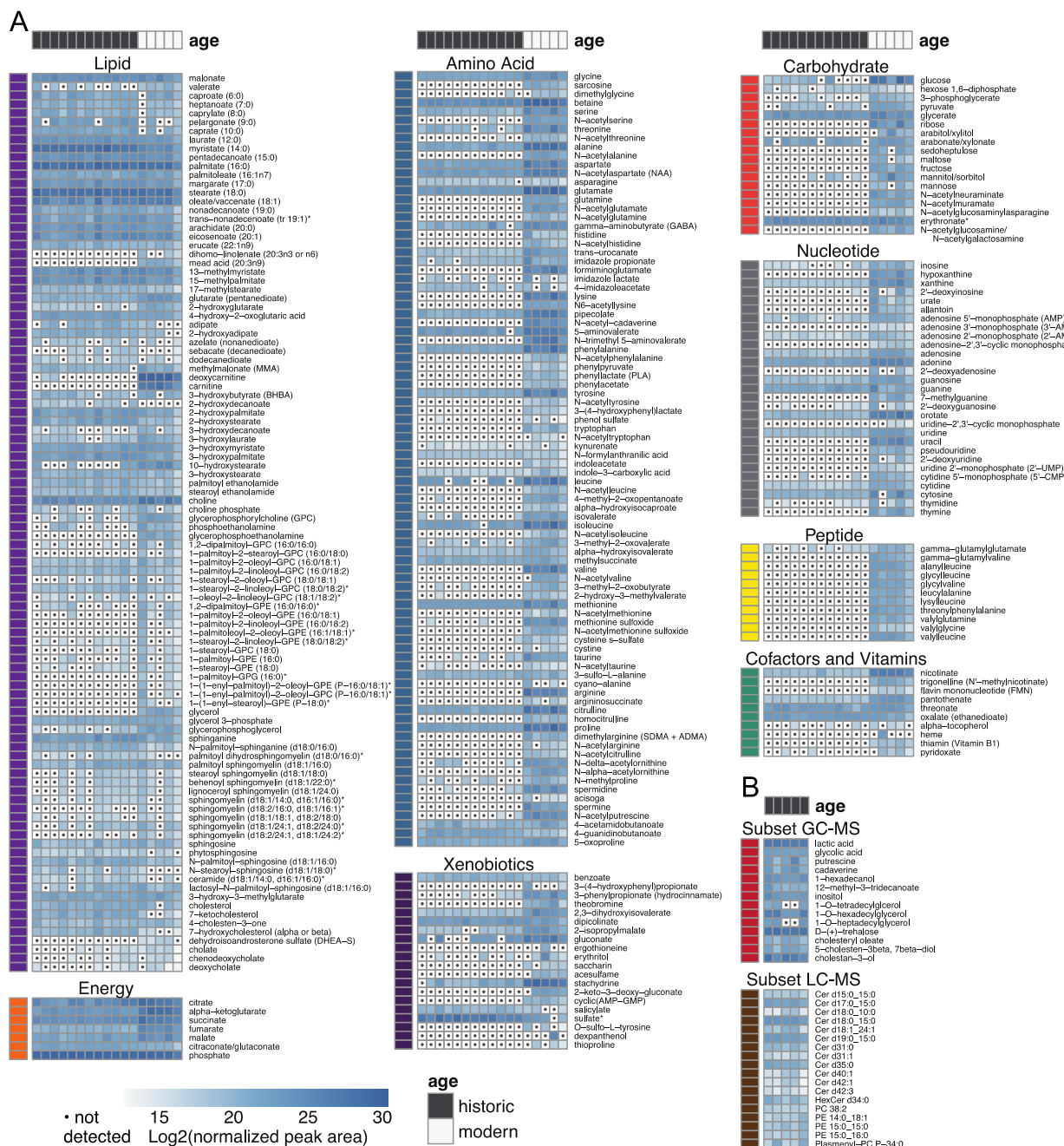
Fig. 1 Heat map summary of metabolites observed in modern and historic dental. Metabolites were quantified by area under the curve and normalized to mass of sample extracted. **a** UPLC-MS/MS-detected metabolites. Samples were hierarchically clustered, and log2 transformed values are presented above, grouped by super-pathway. **b** Metabolites detected by GC-MS and LC-MS in historic calculus. Non-filled cells containing a dot indicate the compound was not detected.

574

16

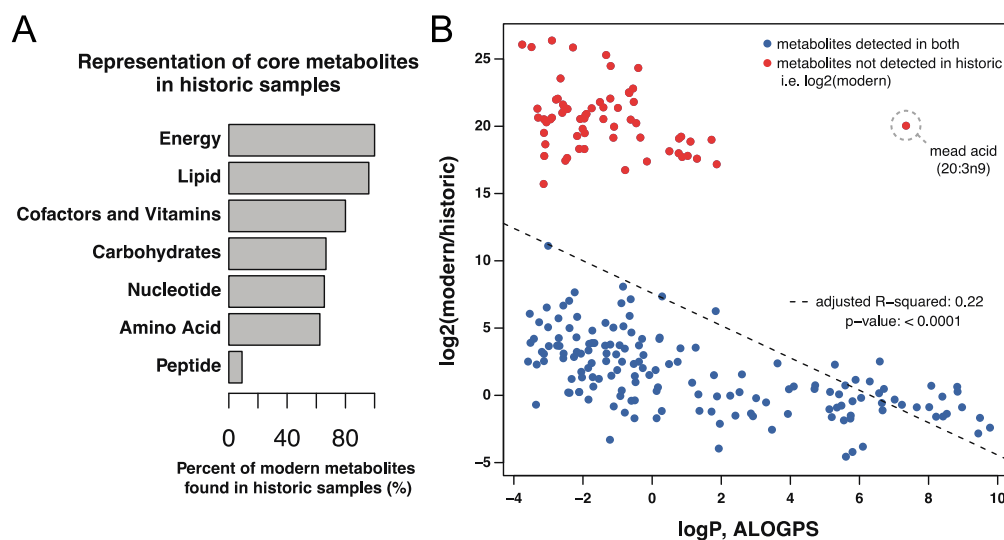**Fig. 2 Compound preservation is correlated with aqueous solubility. a** Percent of high ubiquity metabolites in modern calculus that were also recovered in at least one historic calculus sample. *Peptides* exhibit the poorest representation in historic dental calculus, with only 9% of the peptides observed to be present in all five modern calculus samples also detected in any historic sample. By contrast, *Lipids* and *Energy* (TCA cycle) super-pathways exhibit high representation in historic calculus, with >96% of compounds found in all five modern samples also recovered from historic dental calculus. *Xenobiotics*, which largely comprise dietary and pharmaceutical compounds, are not shown. **b** The log2 fold-change (modern/historic) of metabolite abundance vs. the 1-octanol vs. water partition coefficient (logP), estimated with the ALOGPS tool. In the cases where metabolites were only detected in modern calculus, the log2 values (not fold-change) were plotted relative to logP. The fitted linear model showed a significant effect ($p<0.0001$) of logP on metabolite fold-change with and adjusted R^2 of 0.22. The outlier from this trend was mead acid (20:3n9).

590
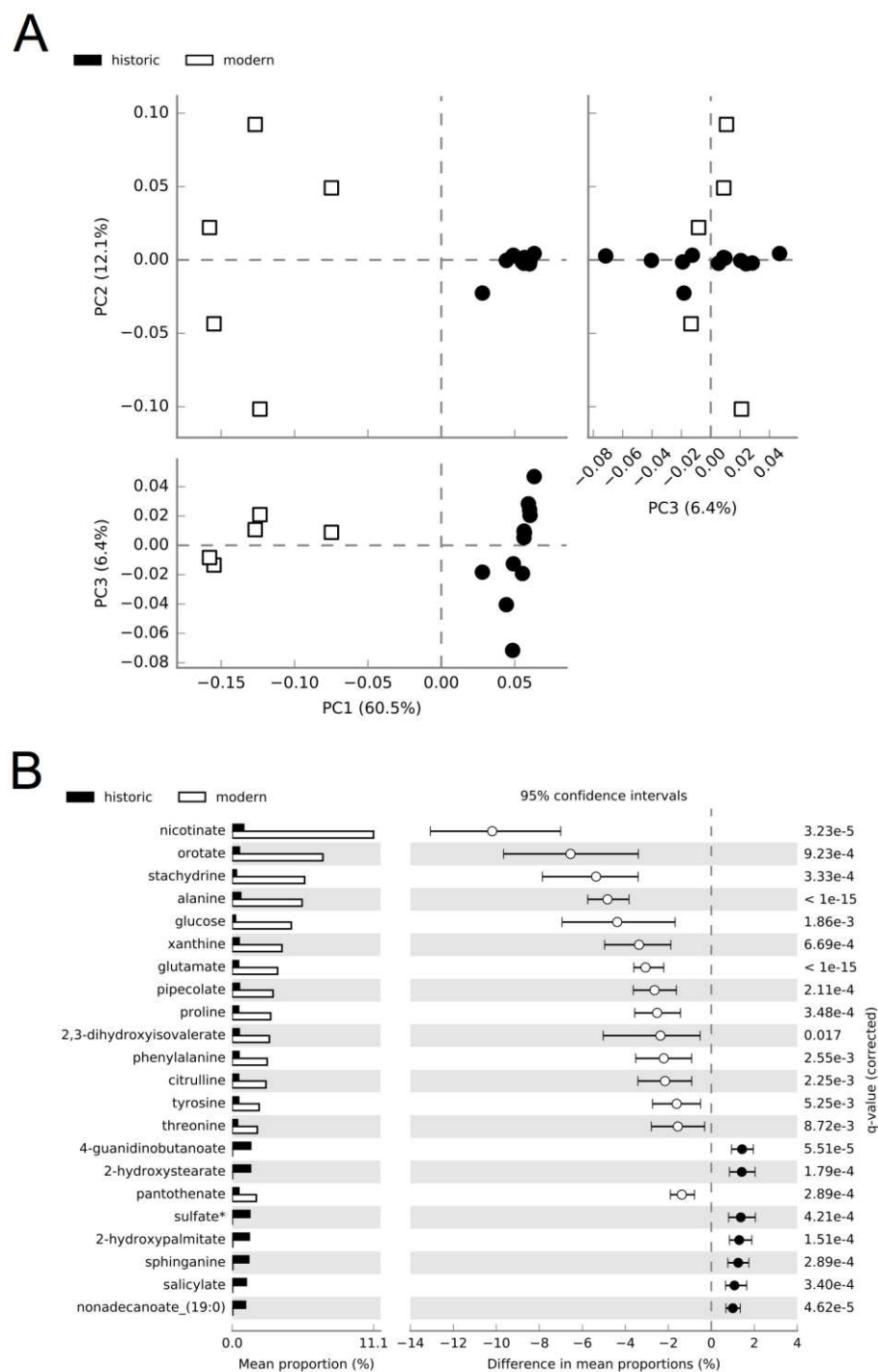
591
592 **Fig. 3** Differences exist in mean proportions of metabolites detected in at least one historic and
593 one modern dental calculus sample. **a** Principal components analysis distinctly separates modern
594 and historic calculus samples. **b** Metabolites with significant differences (q ≤ 0.05, effect size of
595 ≥1.0) in mean proportions between historic and modern calculus.
596
597

18

Fig. 4 Differences exist in proportions of super-pathways, sub-pathways, and metabolites represented in at least one historic and one modern dental calculus sample. Significantly different (q ≤ 0.05, effect size of ≥1.0) proportions of **a** Super-pathways, **b** Sub-pathways, and **c** metabolites. Individual metabolites between historic and modern samples.
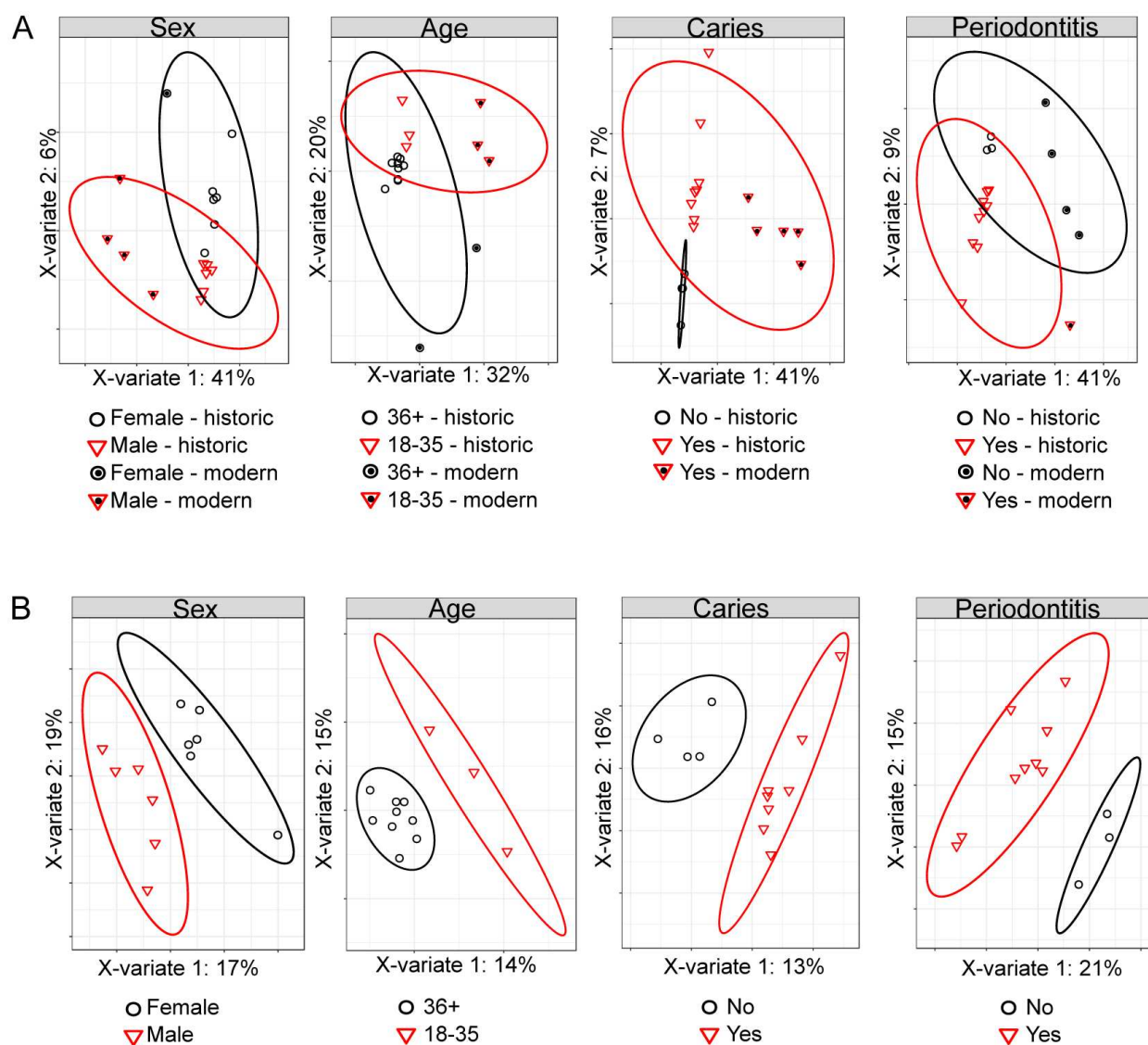
Fig. 5 Partial least squares discriminant analysis of metabolites detected at least one modern and one historic calculus sample. **a** Calculus samples cluster based on time period rather than biological category (sex, age, caries status and periodontal disease status) when including all metabolites detected in at least one modern and one historic sample. **b** Historic calculus samples cluster based on biological category (sex, age, caries status and periodontal disease status) when including all metabolites detected in at least one historic sample. Ellipses indicate 95% confidence intervals.

20

Supplementary Tables

Table S1. Raw UPLC-MS/MS data from Metabolon. Tab 1 (OrigScale) contains data normalized in terms of raw area counts. Tab 2 (MassNormImp) contains data normalized as follows: values for each sample are normalized by sample mass available/utilized for extraction, then each biochemical is rescaled to set the median equal to 1, and missing values are imputed with the minimum. (Excel sheet).

Table S2. Raw Data from the University of Wisocnson-Madison. Tab 1 Metabolites detected by GC-MS. Tab 2 Metabolites detected by UPLC-MS/MS. (Excel sheet).

Table S3. Differential abundance of UPLC-MS/MS-identified metabolites between modern and historic dental calculus. (Word doc).

Table S4. Q2 values for all PLS-DAs.

Supplementary Figures

Fig. S1 Historic calculus samples contain oral bacterial community profiles. **a** Historic calculus on teeth from CS18 prior to sampling. **b** Percent of bacterial community in calculus samples attributable to distinct environmental sources by SourceTracker analysis. Modern samples from Ziesemer et al. (2015), demonstrate that a high proportion of the microbial community assigned to an "Unknown" source is characteristic of dental calculus. CS6 failed to build DNA libraries with the AccuPrimePFX polymerase.

Fig. S2 Comparison of quantified metabolites from samples analyzed by Metabolon, Inc. and Wisconsin-Madison. Five calculus samples were analyzed by GC-MS and LC-MS in Madison, Wisconsin; the relative quantitation obtained on these methods was significantly correlated with results from Metabolon, Inc. (linear regression, p < 0.001).

Fig. S3. Representation of diverse metabolic pathways preserved in calculus. Large circles represent metabolites identified in calculus. Black rings around large circles indicate the metabolite was detected in historic calculus.

Fig. S4. Representation of pathways for biosynthesis of secondary metabolites preserved in calculus. Large circles represent metabolites identified in calculus. Black rings around large circles indicate the metabolite was detected in historic calculus.

Fig. S5 Global Natural Products Social Molecular Networking (GNPS) analysis of UPLC-MS/MS spectra (Wisconsin subset) clusters compounds containing phosphocholine head groups. This network of molecular clusters (nodes) contains molecules with putative identifications (dark blue) to phosphatidylcholines and sphingomyelins containing phosphocholine. The edges denote at least 3 matching fragments between spectra and a cosine score of >0.8.

Fig. S6. Differences exist in mean proportions of metabolites universally detected in all historic and modern dental calculus samples. **a** Principal components analysis distinctly separates

21

662 modern and historic calculus samples. **b** Metabolites with significant differences (q ≤ 0.05, effect
663 size of ≥1.0) in mean proportions between historic and modern calculus.

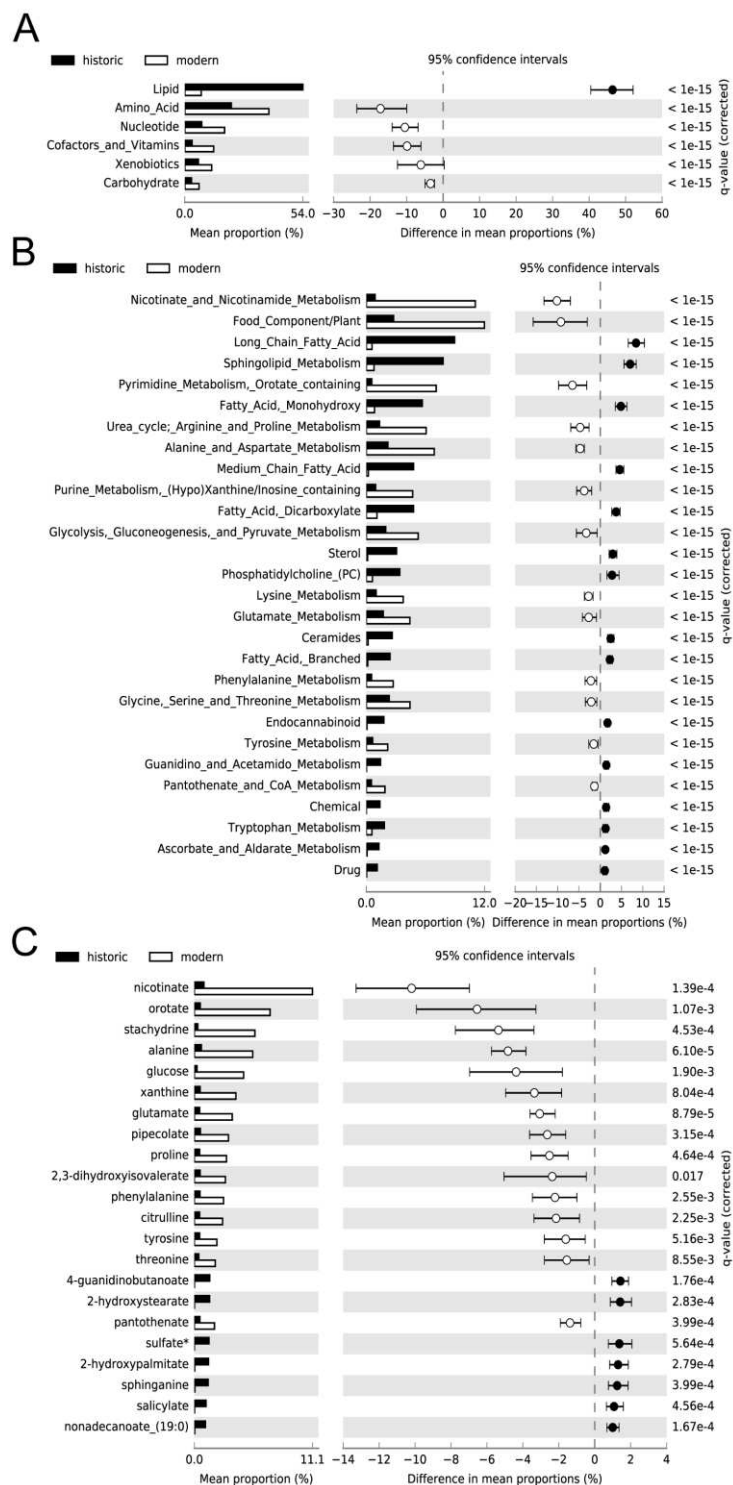664

665 **Fig. S7.** Differences exist in proportions of super-pathways, sub-pathways, and metabolites
666 universally detected in all historic and modern dental calculus samples. Significantly different (q
667 ≤ 0.05, effect size of ≥1.0) proportions of **a** Super-pathways, **b** Sub-pathways, and **c** Individual
668 metabolites between historic and modern samples.

669

670 **Fig. S8.** Partial least squares discriminant analysis of metabolites universally present in calculus
671 samples. **a** Calculus samples cluster based on time period rather than biological category (sex,
672 age, caries status and periodontal disease status) when including metabolites detected in all
673 seventeen calculus samples. **b** Historic calculus samples cluster based on biological category
674 (sex, age, caries status and periodontal disease status) when including metabolites detected in all
675 twelve historic samples. **c** When using only universally detected metabolites in the *Lipid* and
676 *Energy* categories (pathways with the best representation in historic samples), it was still not
677 possible to discriminate samples based on biological category, although the separation between
678 historic and modern samples was reduced slightly compared to **a**. Ellipses indicate 95%
679 confidence intervals.

680

681 **Fig. S9.** Comparison of sulfate abundance and the relative abundance of the oral sulfate-
682 producing genus, *Methanobrevibacter*, shown using **a** linear and **b** log scales.
683 *Methanobrevibacter* relative abundance was estimated using 16S rRNA gene sequence counts,
684 and no correlation was observed with sulfate abundance. *Methanobrevibacter* was not detected
685 in CS18.

22

References

Atkinson, W., Downer, P., Lever, M., Chambers, S. T., & George, P. M. (2007). Effects of orange juice and proline betaine on glycine betaine and homocysteine in healthy male subjects. *European Journal of Nutrition*, *46*(8), 446–452. doi:10.1007/s00394-007-0684-5

Badri, D. V., & Vivanco, J. M. (2009). Regulation and function of root exudates. *Plant, Cell & Environment*, *32*(6), 666–681. doi:10.1111/j.1365-3040.2009.01926.x

Barnes, V. M., Ciancio, S. G., Shibly, O., Xu, T., Devizio, W., Trivedi, H. M., et al. (2011). Metabolomics Reveals Elevated Macromolecular Degradation in Periodontal Disease. *Journal of Dental Research*, *90*(11), 1293–1297. doi:10.1177/0022034511416240

Barnes, V. M., Teles, R., Trivedi, H. M., Devizio, W., Xu, T., Mitchell, M. W., et al. (2009). Acceleration of purine degradation by periodontal diseases. *Journal of Dental Research*, *88*(9), 851–855. doi:10.1177/0022034509341967

Bartold, P. M., & Van Dyke, T. E. (2013). Periodontitis: a host-mediated disruption of microbial homeostasis. Unlearning learned concepts. *Periodontology 2000*, *62*, 203–217.

Beger, R. D. (2013). A review of applications of metabolomics in cancer. *Metabolites*, *3*(3), 552–574. doi:10.3390/metabo3030552

Bennett, M., & Gilroy, D. W. (2016). Lipid Mediators in Inflammation. *Microbiology Spectrum*, *4*(6). doi:10.1128/microbiolspec.MCHD-0035-2016

Blatt, S. H., Redmond, B. G., Cassman, V., & Sciulli, P. W. (2011). Dirty teeth and ancient trade: Evidence of cotton fibres in human dental calculus from Late Woodland, Ohio. *International Journal of Osteoarchaeology*, *21*(6), 669–678. doi:10.1002/oa.1173

Bouatra, S., Aziat, F., Mandal, R., Guo, A. C., Wilson, M. R., Knox, C., et al. (2013). The human urine metabolome. *PLoS ONE*, *8*(9), e73076. doi:10.1371/journal.pone.0073076

Brooks, S., & Suchey, J. M. (1990). Skeletal age determination based on the os pubis: A comparison of the Acsádi-Nemeskéri and Suchey-Brooks methods. *Human Evolution*, *5*(3), 227–238. doi:10.1007/BF02437238

Buckberry, J. L., & Chamberlain, A. T. (2002). Age estimation from the auricular surface of the ilium: A revised method. *American Journal of Physical Anthropology*, *119*(3), 231–239. doi:10.1002/ajpa.10130

Buckley, S., Usai, D., Jakob, T., Radini, A., & Hardy, K. (2014). Dental Calculus Reveals Unique Insights into Food Items, Cooking and Plant Processing in Prehistoric Central Sudan. *PLoS ONE*, *9*(7), e100808–10. doi:10.1371/journal.pone.0100808

Caporaso, J. G., Kuczynski, J., Stombaugh, J., Bittinger, K., Bushman, F. D., Costello, E. K., et al. (2010). QIIME allows analysis of high-throughput community sequencing data. *Nature Methods*, *7*(5), 335–336. doi:10.1038/nmeth.f.303

Cappellini, E., Jensen, L. J., Szklarczyk, D., Ginolhac, A., da Fonseca, R. A. R., Stafford, T. W., et al. (2012). Proteomic analysis of a pleistocene mammoth femur reveals more than one hundred ancient bone proteins. *Journal of Proteome Research*, *11*(2), 917–926. doi:10.1021/pr200721u

Castillo-García, M. L., Aguilar-Caballos, M. P., & Gómez-Hens, A. (2015). Determination of acetylsalicylic acid and its major metabolites in bovine urine using ultra performance liquid chromatography. *Journal of Chromatography B*, *985*, 85–90. doi:10.1016/j.jchromb.2015.01.026

Cosgrove, J. P., Church, D. F., & Pryor, W. A. (1987). The kinetics of the autoxidation of polyunsaturated fatty acids. *Lipids*, *22*(5), 299–304.

23

732 Crisp, M., Demarchi, B., Collins, M., Morgan-Williams, M., Pilgrim, E., & Penkman, K. (2013).
733   Isolation of the intra-crystalline proteins and kinetic studies in Struthio camelus (ostrich)
734   eggshell for amino acid geochronology. *Quaternary Geochronology*, *16*, 110–128.
735   doi:10.1016/j.quageo.2012.09.002
736 Dame, Z. T., Aziat, F., Mandal, R., Krishnamurthy, R., Bouatra, S., Borzouie, S., et al. (2015).
737   The human saliva metabolome. *Metabolomics*, *11*(6), 1864–1883. doi:10.1007/s11306-015-
738   0840-5
739 Darveau, R. P., Pham, T. T. T., Lemley, K., Reife, R. A., Bainbridge, B. W., Coats, S. R., et al.
740   (2004). *Porphyromonas gingivalis* Lipopolysaccharide Contains Multiple Lipid A Species
741   That Functionally Interact with Both Toll-Like Receptors 2 and 4. *Infection and Immunity*,
742   *72*(9), 5041–5051. doi:10.1128/IAI.72.9.5041-5051.2004
743 Daskalaki, E., Blackburn, G., Kalna, G., Zhang, T., Anthony, N., & Watson, D. (2015). A Study
744   of the Effects of Exercise on the Urinary Metabolome Using Normalisation to Individual
745   Metabolic Output. *Metabolites*, *5*(1), 119–139. doi:10.3390/metabo5010119
746 Edgar, R. C. (2010). Search and clustering orders of magnitude faster than BLAST.
747   *Bioinformatics*, *26*(19), 2460–2461. doi:10.1093/bioinformatics/btq461
748 Ferembach, D., Schwindezky, I., & Stoukal, M. (1980). Recommendation for Age and Sex
749   Diagnoses of Skeletons. *Journal of Human Evolution*, *9*, 517–549.
750 Fleet, J. C., Gliniak, C., Zhang, Z., Xue, Y., Smith, K. B., McCreedy, R., & Adedokun, S. A.
751   (2008). Serum metabolite profiles and target tissue gene expression define the effect of
752   cholecalciferol intake on calcium metabolism in rats and mice. *The Journal of Nutrition*,
753   *138*(6), 1114–1120.
754 Foley, J. D., III, Sneed, J. D., Steinhubl, S. R., Kolasa, J., Ebersole, J. L., Lin, Y., et al. (2012).
755   Oral fluids that detect cardiovascular disease biomarkers. *Oral Surgery, Oral Medicine, Oral
756   Pathology and Oral Radiology*, *114*(2), 207–214. doi:10.1016/j.oooo.2012.03.003
757 Frantz, L. A. F., Mullin, V. E., Pionnier-Capitan, M., Lebrasseur, O., Ollivier, M., Perri, A., et al.
758   (2016). Genomic and archaeological evidence suggest a dual origin of domestic dogs.
759   *Science*, *352*(6290), 1228–1231. doi:10.1126/science.aaf3161
760 Gao, B., & Gupta, R. S. (2012). Phylogenetic framework and molecular signatures for the main
761   clades of the phylum Actinobacteria. *Microbiology and Molecular Biology Reviews*, *76*(1),
762   66–112. doi:10.1128/MMBR.05011-11
763 Hahn, T. J., Hendin, B. A., Scharp, C. R., & Haddad, J. G. (1972). Effect of chronic
764   anticonvulsant therapy on serum 25-hydroxycalciferol levels in adults. *The New England
765   Journal of Medicine*, *287*(18), 900–904. doi:10.1056/NEJM197211022871803
766 Hardy, K., Buckley, S., Collins, M. J., Estalrrich, A., Brothwell, D., Copeland, L., et al. (2012).
767   Neanderthal medics? Evidence for food, cooking, and medicinal plants entrapped in dental
768   calculus. *Die Naturwissenschaften*, *99*(8), 617–626. doi:10.1007/s00114-012-0942-0
769 Hardy, K., Radini, A., Buckley, S., Sarig, R., Copeland, Les, Gopher, A., & Barkai, R. (2016).
770   Dental calculus reveals potential respiratory irritants and ingestion of essential plant-based
771   nutrients at Lower Palaeolithic Qesem Cave Israel. *Quaternary International*, *398*(c), 129–
772   135. doi:10.1016/j.quaint.2015.04.033
773 Hillson, S. (1996). *Dental Anthropology*. Cambridge: Cambridge University Press.
774   doi:10.1017/CBO9781139170697
775 Jensen, M. K., Bertoia, M. L., Cahill, L. E., Agarwal, I., Rimm, E. B., & Mukamal, K. J. (2014).
776   Novel metabolic biomarkers of cardiovascular disease. *Nature Reviews Endocrinology*,
777   *10*(11), 659–672. doi:10.1038/nrendo.2014.155

24

778 Klugh, K. R., & Cumming, J. R. (2007). Variations in organic acid exudation and aluminum
779   resistance among arbuscular mycorrhizal species colonizing Liriodendron tulipifera. *Tree*
780   *Physiology*, *27*(8), 1103–1112. doi:10.1093/treephys/27.8.1103
781 Knights, D., Kuczynski, J., Charlson, E. S., Zaneveld, J., Mozer, M. C., Collman, R. G., et al.
782   (2011). Bayesian community-wide culture-independent microbial source tracking. *Nature*
783   *Methods*, *8*(9), 761–763. doi:10.1038/nmeth.1650
784 Kuboniwa, M., Sakanaka, A., Hashino, E., Bamba, T., Fukusaki, E., & Amano, A. (2016).
785   Prediction of Periodontal Inflammation via Metabolic Profiling of Saliva. *Journal of Dental*
786   *Research*, *95*(12), 1381–1386. doi:10.1177/0022034516661142
787 Lankinen, M., Kolehmainen, M., Jääskeläinen, T., Paananen, J., Joukamo, L., Kangas, A. J., et
788   al. (2014). Effects of whole grain, fish and bilberries on serum metabolic profile and lipid
789   transfer protein activities: a randomized trial (Sysdimet). *PLoS ONE*, *9*(2), e90352.
790   doi:10.1371/journal.pone.0090352
791 Lever, M., Sizeland, P.C.B., Bason, L. M., Hayman, C. M., & Chambers, S. T. (1994). Glycine
792   betine and proline betaine in human blood and urine. *Biochimica et biophysica acta*, *1200*,
793   259–264.
794 Lovejoy, C. O., Meindl, R. S., Pryzbeck, T. R., & Mensforth, R. P. (1985). Chronological
795   metamorphosis of the auricular surface of the ilium: A new method for the determination of
796   adult skeletal age at death. *American Journal of Physical Anthropology*, *68*(1), 15–28.
797   doi:10.1002/ajpa.1330680103
798 López-Lara, I. M., & Geiger, O. (2016). Bacterial lipid diversity. *Biochimica et biophysica acta*.
799   doi:10.1016/j.bbalip.2016.10.007
800 Meyer, M., Kircher, M., Gansauge, M.-T., Li, H., Racimo, F., Mallick, S., et al. (2012). A high-
801   coverage genome sequence from an archaic Denisovan individual. *Science*, *338*(6104), 222–
802   226. doi:10.1126/science.1224344
803 Nagana Gowda, G. A., Gowda, Y. N., & Raftery, D. (2015). Massive glutamine cyclization to
804   pyroglutamic acid in human serum discovered using NMR spectroscopy. *Analytical*
805   *chemistry*, *87*(7), 3800–3805. doi:10.1021/ac504435b
806 Nishizuka, Y. (1995). Protein kinase C and lipid signaling for sustained cellular responses. *The*
807   *FASEB Journal*, *9*(7), 484–496. doi:10.1096/fj.1530-6860
808 Oakley, L. H., Casadio, F., Shull, K. R., & Broadbelt, L. J. (2015). Microkinetic modeling of the
809   autoxidative curing of an alkyd and oil-based paint model system. *Applied Physics A*, *121*(3),
810   869–878. doi:10.1007/s00339-015-9363-1
811 Ogden, A. (2005). A New and Simple System for the Recording of Periodontal Disease in
812   Skeletal Material (pp. 1–1). Presented at the British Association for Biological Anthropology
813   and Osteoarchaeology.
814 Parks, D. H., & Beiko, R. G. (2010). Identifying biologically relevant differences between
815   metagenomic communities. *Bioinformatics*, *26*(6), 715–721.
816   doi:10.1093/bioinformatics/btq041
817 Parks, D. H., Tyson, G. W., Hugenholtz, P., & Beiko, R. G. (2014). STAMP: statistical analysis
818   of taxonomic and functional profiles. *Bioinformatics*, *30*(21), 3123–3124.
819   doi:10.1093/bioinformatics/btu494
820 Phenice, T. W. (1969). A newly developed visual method of sexing the os pubis. *American*
821   *Journal of Physical Anthropology*, *30*(2), 297–301. doi:10.1002/ajpa.1330300214
822 Psychogios, N., Hau, D. D., Peng, J., Guo, A. C., Mandal, R., Bouatra, S., et al. (2011). The
823   human serum metabolome. *PLoS ONE*, *6*(2), e16957. doi:10.1371/journal.pone.0016957

824 Radini, A., Buckley, S., Rosas, A., Estalrrich, A., la Rasilla, de, M., & Hardy, K. (2016).
825   Neanderthals, trees and dental calculus: new evidence from El Sidroń. *Antiquity*, *90*(350),
826   290–301. doi:10.15184/aqy.2016.21
827 Rawlins, B. G., McGrath, S. P., Scheib, A., Breward, N., Cave, M. R., Lister, B., et al. (2012).
828   *The advanced soil geochemical atlas of England and Wales*. British Geological Survey.
829 Rohart, F., Gautier, B., Singh, A., & Le Cao, K.-A. (2017). mixOmics (draft1): an R package for
830   'omics feature selection and multiple data integration. *bioRxiv*, 108597. doi:10.1101/108597
831 Rustan, A. C., & Drevon, C. A. (2005). *Fatty Acids: Structures and Properties. Encyclopedia of*
832   *Life Sciences*. John Wiley & Sons, Ltd. doi:10.1038/npg.els.0003894
833 Sakanaka, A., Kuboniwa, M., Hashino, E., Bamba, T., Fukusaki, E., & Amano, A. (2017).
834   Distinct signatures of dental plaque metabolic byproducts dictated by periodontal
835   inflammatory status. *Scientific Reports*, *7*, 42818. doi:10.1038/srep42818
836 Schwartz, J. H. (1996). Skeleton keys: An introduction to human skeletal morphology,
837   development, and analysis. *Oxford Univeristy Press*. doi:10.1007/BF02735270
838 Scully, C., el-Maaytah, M., Porter, S. R., & Greenman, J. (1997). Breath odor: etiopathogenesis,
839   assessment and management. *European Journal of Oral Sciences*, *105*(4), 287–293.
840 Skoglund, P., Ersmark, E., Palkopoulou, E., & Dalén, L. (2015). Ancient wolf genome reveals an
841   early divergence of domestic dog ancestors and admixture into high-latitude breeds. *Current*
842   *biology : CB*, *25*(11), 1515–1519. doi:10.1016/j.cub.2015.04.019
843 Skoglund, P., Storå, J., Götherström, A., & Jakobsson, M. (2013). Accurate sex identification of
844   ancient human remains using DNA shotgun sequencing. *Journal of Archaeological Science*,
845   *40*(12), 4477–4482. doi:10.1016/j.jas.2013.07.004
846 Sugimoto, M., Wong, D. T., Hirayama, A., Soga, T., & Tomita, M. (2010). Capillary
847   electrophoresis mass spectrometry-based saliva metabolomics identified oral, breast and
848   pancreatic cancer-specific profiles. *Metabolomics*, *6*(1), 78–95. doi:10.1007/s11306-009-
849   0178-y
850 Sysi-Aho, M., Ermolov, A., Gopalacharyulu, P. V., Tripathi, A., Seppänen-Laakso, T.,
851   Maukonen, J., et al. (2011). Metabolic regulation in progression to autoimmune diabetes.
852   *PLoS Computational Biology*, *7*(10), e1002257. doi:10.1371/journal.pcbi.1002257
853 Takahashi, N. (2015). Oral Microbiome Metabolism: From "Who Are They?" to "What Are
854   They Doing?." *Journal of Dental Research*.
855 Takahashi, N., Washio, J., & Mayanagi, G. (2010). Metabolomics of Supragingival Plaque and
856   Oral Bacteria. *Journal of Dental Research*, *89*(12), 1383–1388.
857   doi:10.1177/0022034510377792
858 Takeda, I., Stretch, C., Barnaby, P., Bhatnager, K., Rankin, K., Fu, H., et al. (2009).
859   Understanding the human salivary metabolome. *NMR in Biomedicine*, *22*(6), 577–584.
860   doi:10.1002/nbm.1369
861 Tetko, I. V., & Bruneau, P. (2004). Application of ALOGPS to predict 1-octanol/water
862   distribution coefficients, logP, and logD, of AstraZeneca in-house database. *Journal of*
863   *Pharmaceutical Sciences*, *93*(12), 3103–3110. doi:10.1002/jps.20217
864 Velasco, J., & Dobarganes, C. (2002). Oxidative stability of virgin olive oil - Velasco - 2002 -
865   European Journal of Lipid Science and Technology - Wiley Online Library. *European*
866   *Journal of Lipid Science and Technology*, *104*(9-10), 661–676. doi:10.1002/1438-
867   9312(200210)104:9/10<661::AID-EJLT661>3.0.CO;2-D
868 Vos, P., Garrity, G., Jones, D., Krieg, N. R., Ludwig, W., Rainey, F. A., et al. (2011). *Bergey's*
869   *Manual of Systematic Bacteriology*.

870 Wade, W. G. (2013). The oral microbiome in health and disease. *Pharmacological Research*,
871   *69*(1), 137–143. doi:10.1016/j.phrs.2012.11.006

872 Wallner-Liebmann, S., Tenori, L., Mazzoleni, A., Dieber-Rotheneder, M., Konrad, M.,
873   Hofmann, P., et al. (2016). Individual Human Metabolic Phenotype Analyzed by. *Journal of*
874   *Proteome Research*, *15*, 1787–1793.
875   doi:10.1021/acs.jproteome.5b01060/suppl_file/pr5b01060_si_001.pdf

876 Wang, Min, & Hajishengallis, G. (2008). Lipid raft-dependent uptake, signalling and
877   intracellular fate of *Porphyromonas gingivalis* in mouse macrophages. *Cellular*
878   *Microbiology*, *10*(10), 2029–2042. doi:10.1111/j.1462-5822.2008.01185.x

879 Wang, Mingxun, Carver, J. J., Phelan, V. V., Sanchez, L. M., Garg, N., Peng, Y., et al. (2016).
880   Sharing and community curation of mass spectrometry data with Global Natural Products
881   Social Molecular Networking. *Nature biotechnology*, *34*(8), 828–837. doi:10.1038/nbt.3597

882 Warinner, C. (2016). Dental Calculus and the Evolution of the Human Oral Microbiome. *Journal*
883   *of the California Dental Association*, *44*(7), 411–420.

884 Warinner, C., Hendy, J., Speller, C., Cappellini, E., Fischer, R., Trachsel, C., et al. (2014). Direct
885   evidence of milk consumption from ancient human dental calculus. *Scientific Reports*, *4*,
886   7104. doi:10.1038/srep07104

887 Warinner, C., Rodrigues, J. F. M., Vyas, R., Trachsel, C., Shved, N., Grossmann, J., et al. (2014).
888   Pathogens and host immunity in the ancient human oral cavity. *Nature Genetics*, *46*(4), 336–
889   344. doi:10.1038/ng.2906

890 Warinner, C., Speller, C., & Collins, M. J. (2015). A new era in palaeomicrobiology: prospects
891   for ancient dental calculus as a long-term record of the human oral microbiome. *Phil*. *Trans*.
892   *R*. *Soc*. *B*, *370*, 20130376.

893 White, D. J. (1991). Processes contributing to the formation of dental calculus. *Biofouling*, *4*(1-
894   3), 209–218. doi:10.1080/08927019109378211

895 Wishart, D. S., Jewison, T., Guo, A. C., Wilson, M., Knox, C., Liu, Y., et al. (2013). HMDB
896   3.0—The Human Metabolome Database in 2013. *Nucleic Acids Research*, *41*(D1), D801–
897   D807. doi:10.1093/nar/gks1065

898 Xavier, A. M., Anunciato, A. K. O., Rosenstock, T. R., & Glezer, I. (2016). Gene Expression
899   Control by Glucocorticoid Receptors during Innate Immune Responses. *Frontiers in*
900   *Endocrinology*, *7*, 31. doi:10.3389/fendo.2016.00031

901 Xia, Y.-Q., Patel, S., Bakhtiar, R., Franklin, R. B., & Doss, G. A. (2005). Identification of a new
902   source of interference leached from polypropylene tubes in mass-selective analysis. *Journal*
903   *of the American Society for Mass Spectrometry*, *16*(3), 417–421.
904   doi:10.1016/j.jasms.2004.11.020

905 Yamada, T., Letunic, I., Okuda, S., Kanehisa, M., & Bork, P. (2011). iPath2.0: interactive
906   pathway explorer. *Nucleic Acids Research*, *39*(suppl), W412–W415. doi:10.1093/nar/gkr313

907 Yan, S.-K., Wei, B.-J., Lin, Z.-Y., Yang, Y., Zhou, Z.-T., & Zhang, W.-D. (2008). A
908   metabonomic approach to the diagnosis of oral squamous cell carcinoma, oral lichen planus
909   and oral leukoplakia. *Oral Oncology*, *44*(5), 477–483.
910   doi:10.1016/j.oraloncology.2007.06.007

911 Yung, P. T., Shafaat, H. S., Connon, S. A., & Ponce, A. (2007). Quantification of viable
912   endospores from a Greenland ice core. *FEMS Microbiology Ecology*, *59*(2), 300–306.
913   doi:10.1111/j.1574-6941.2006.00218.x

914 Zalba, S., & Hagen, Ten, T. L. M. (2017). Cell membrane modulation as adjuvant in cancer
915   therapy. *Cancer treatment reviews*, *52*, 48–57. doi:10.1016/j.ctrv.2016.10.008

916 Zhang, A., Sun, H., & Wang, X. (2012). Saliva Metabolomics Opens Door to Biomarker
917   Discovery, Disease Diagnosis, and Treatment. *Applied Biochemistry and Biotechnology*,
918   *168*(6), 1718–1727. doi:10.1007/s12010-012-9891-5
919 Ziesemer, K. A., Mann, A. E., Sankaranarayanan, K., Schroeder, H., Ozga, A. T., Brandt, B. W.,
920   et al. (2015). Intrinsic challenges in ancient microbiome reconstruction using 16S rRNA
921   gene amplification. *Scientific Reports*, *5*, 16498–19. doi:10.1038/srep16498
922